Title: Aggregation inhibits alpha-synuclein dephosphorylation resulting in the observation of pathological enrichment

Authors:

Choi SG[1], Garcia-Prada D. [1],Tittle T. [1], Kordower JH[2], Melki R[3], Killinger BA[1]

[1]Department of Neurological Sciences, Rush University Medical Center, Chicago, IL, USA.

[2]ASU-Banner Neurodegenerative Disease Research Center and School of Life Sciences, Arizona State University, Tempe, AZ, USA.

[3]Institut Francois Jacob (MIRCen), CEA and Laboratory of Neurodegenerative Diseases, CNRS, Fontenay-Aux-Roses Cedex, France.

Abstract

Alpha-synuclein is an intrinsically disordered protein that aggregates in the brain in several neurodegenerative diseases collectively called synucleinopathies. Phosphorylation of alpha-synuclein (αsyn) at serine 129 (PSER129) was considered rare in the healthy human brain but is enriched in pathological αsyn aggregates and is used as a specific marker for disease inclusions. However, recent observations challenge this assumption by demonstrating that PSER129 results from neuronal activity and can be readily detected in the non-diseased mammalian brain. Here, we tested experimental conditions under which two distinct PSER129 pools, endogenous-PSER129 and aggregated-PSER129, could be detected and differentiated in the brain. Results showed that in the mouse brain, perfusion fixation conditions greatly influenced detection of endogenous-PSER129, with endogenous-PSER129 being nearly undetectable after delayed perfusion fixation (30min and 1hr post-mortem interval). Exposure to anesthetics (e.g., ketamine and xylazine) before perfusion did not significantly influence endogenous-PSER129 detection or levels. In situ, non-specific phosphatase (i.e., calf alkaline phosphatase, CIAP) selectively dephosphorylated endogenous-PSER129 while preformed fibril-seeded aggregates and genuine disease aggregates (Lewy pathology and Papp–Lantos bodies in Parkinson's disease and multiple systems atrophy brain, respectively) were resistant to CIAP-mediated dephosphorylation. Phosphatase resistance of aggregates was abolished by sample denaturation. We conclude that in the mammalian brain, there is an abundant steady state of endogenous-PSER129, and PSER129 association with pathology is, at least partially, due to dephosphorylation resistance of αsyn aggregates. Our findings have implications for the mechanism of PSER129-accumulation in the synucleinopathy brain.

Introduction

Synucleinopathies are age-related neurodegenerative diseases, including Parkinson's disease (PD), Dementia with Lewy bodies (DLB), and Multiple System Atrophy (MSA) where the prominent neuropathological hallmark is aggregates of misfolded alpha-synuclein (αsyn) protein (1). Numerous potential mechanisms for αsyn aggregation have been described, but many details, particularly within the human diseased brain, remain unclear. Understanding cellular and molecular mechanisms driving αsyn misfolding and aggregation is fundamental for understanding synucleinopathy disease origins and progression.

Fujiwara et al. 2002 identified αsyn phosphorylated at serine 129 (PSER129) within αsyn aggregates from PD, DLB and MSA brain (2). Numerous other post-translational modifications (PTMs) associated with αsyn aggregates have been identified (3) with many of these PTMs occurring following alpha-synuclein aggregation (4). In the PD brain, nearly all the αsyn in brain aggregates is PSER129 (~90%)(2), while endogenous-PSER129 levels in the healthy brain have been estimated to be much less (<5%). However, recent reports suggest that PSER129 occurs during normal neuronal activity (5) and is abundant in specific brain regions (6). PSER129 may have functional significance by regulating αsyn interactions (7), αsyn-subcellular localization (6), or αsyn-turnover (8, 9). PSER129 functional significance for disease is unclear, but determining if PSER129 plays a protective(10), neutral(11, 12), or toxic role (13) in the αsyn aggregation processes is important for understanding fundamental synucleinopathy disease mechanisms.

PSER129 detection in the healthy mammalian brain (i.e., endogenous-PER129) has been inconsistent across studies (7, 14-16) with varying abundance, cellular localization, and regional distribution. We observed high variability in the steady-state level of endogenous-PSER129 that could be explained by either sample preparation or biological factors such as neuronal activity (5). Protein phosphorylation is highly dynamic, cycling between phosphorylation and dephosphorylated forms on small timescales, and as a result accurate measurement of PTM's require that biological processes in tissues are rapidly inhibited whether by perfusion fixation or other

techniques (e.g., flash freezing, small molecule enzyme inhibitors etc.)(17). It's unclear whether variability in endogenous-PSER129 is due to protocol differences or an unknown biological variable.

Results

Rapid perfusion fixation preserves endogenous-PSER129

To investigate why endogenous-PSER129 detection is variable across studies, we performed delayed perfusion fixation of CO2 euthanized mice. To do this, after death we immediately removed the animal's blood by perfusion and then delayed the time until perfusion with PFA was performed. We found (Fig. 1A-C) PSER129 was readily detectable and abundant in brain regions we've previously described (6) in mice rapidly perfused after death (<30s). In contrast, 30-min delayed perfusion resulted in dramatically reduced PSER129, with only a few PSER129 positive nuclei being detectable in a few brain regions, including the olfactory bulb and hippocampus. Similarly, 60-min delayed perfusion resulted in reduced PSER129 staining, with weak reactivity in some cell nuclei of the olfactory bulb and hippocampus. Quantitative western blots showed that the total amount of αsyn was not significantly altered following delayed perfusion fixation, but PSER129 levels were markedly reduced ($F(2,7) = 38.29$, $p=0.0002$) at 30-min delayed (Optimal vs. 30-min, -97.23% ±0.122), and 60-min (Optimal vs. 60-min, -97.9% ±0.122)(Fig. 1D-F). The distribution of total protein looked similar between all samples (Fig. 1D, left panel). Similar patterns of high molecular weight species (i.e., >30kda) were observed for both PSER129 and αsyn (Fig. 1D, right panels). High molecular weight PSER129 appeared less sensitive to delayed fixation than 15kDa PSER129.

Anesthesia exposure does not influence PSER129 abundance

Ketamine and xylazine are commonly used anesthetics for perfusion and fixation and this procedure could potentially influence endogenous-PSER129 via their effects on neuronal activity(18, 19). To determine if either anesthetic influenced endogenous-PSER129 detection, we performed perfusion fixation on mice acutely exposed to ketamine (100mg/kg), xylazine (10mg/kg), 10 min prior to C02-mediated euthanization.

Results showed that regardless of anesthesia exposure, no significant difference in endogenous-PSER129 content was detected in the mouse brain. IHC detection of PSER129 was similar between groups (Fig. 2A). Quantitative western blot of proteins extracted from PFA-fixed brain sections encompassing the entire brain (Fig. 2B) showed that the amount of αsyn (Fig. 2C), PSER129 (Fig. 2D), or the ratio of PSER129/αsyn (Fig. 2E), did not significantly differ between anesthetic treatments. PSER129 and αsyn quantities were not significantly correlated.

Aggregated-PSER129 selectively resist in situ dephosphorylation

To determine if endogenous-PSER129 could be differentiated from aggregated-PSER129, we pretreated brain tissues from OB-PFF injected mice with calf intestine alkaline phosphatase (CIAP). Without CIAP treatment, PSER129 staining was observed as before (6) throughout the neuroaxis of mice treated with PBS and PFFs (Fig. 3A-C). For OB-PFF mice, pathology bearing regions (i.e., OB, GCL, EC, AMYG) aggregated-PSER129 was difficult to discern from non-aggregated endogenous αsyn, except for regions where endogenous-PSER129 is relatively low (e.g., GCL). CIAP pretreatment resulted in the abolishment of PSER129 staining in PBS mice, while clear PSER129-postive processes and concentric bodies were observed in select brain regions of OB-PFF mice, consistent with aggregation seen in the OB-PFF model (20-22). CIAP-resistant PSER129 was observed in the MCL of OB-PFF mice, which was completely obscured by endogenous-PSER129 when CIAP was not used. We tested several proteases, but despite having predicted cleavage sites adjacent to αsyn Ser129, they did not completely abolish PSER129 staining in the PBS mice (Fig. S1). PK can eliminate endogenous-PSER129(22) (Fig. S1), but the treatment is destructive, limiting its compatibility with common downstream techniques (LC-MS based peptide identification) CIAP is non-destructive and effective, and therefore should be the preferred approach to differentiate endogenous- vs. aggregated-PSER129.

αSyn aggregates in synucleinopathy brain resist in situ dephosphorylation

PSER129 is a selective sensitive marker for pathology in the synucleinopathy brain, as endogenous-PSER129 levels are thought to be low in the non-synucleinopathy brain. Therefore, we tested the hypothesis that αsyn aggregates in the human brain

were CIAP resistant. We stained PSER129 in PD (Fig. 4A,C) and MSA (Fig. 4B,D) midbrain with and without CIAP pretreatment. Without CIAP, as expected, we observed abundant Lewy pathology (Fig. 4C) and Papp Lantos bodies (Fig. 4D) in the PD and MSA brain, respectively. Following CIAP treatment, we observed similar staining in both the PD and MSA brain (Fig. 4C, D, "+CIAP"). Quantification confirmed there was no statistically significant difference in PSER129 staining with or without CIAP pretreatment (Fig 4E).

Denaturation abolishes aggregated-PSER129 CIAP resistance.

Alpha-synuclein conformational transition to aggregates imparts resistance to proteases. PFF seeded (Fig. 3) and bona fide αsyn aggregates (Fig. and 4A-E) resist CIAP-mediated dephosphorylation in situ. To determine if the observed effect was due to the conformation of aggregates, we denatured the brain samples, separated the proteins by WB, and exposed blotted denatured proteins to CIAP. We did this for proteins from untreated WT mice, OB-PFF WT mice, M83 mice, PD midbrain, and MSA midbrain. Results show that in the denatured samples, CIAP abolished reactivity in non-aggregate containing samples (i.e., untreated WT) and aggregate containing samples (i.e., OB-PFF, M83, PD, and MSA). CIAP pretreatment abolished the reactivity of monomeric (14kDa) and high molecular weight species (>30kDa). This shows that conformation imparts resistance to CIAP, analogous to protease-resistance.

Discussion

αSyn aggregation renders it impervious to enzyme-mediated (i.e., CIAP) dephosphorylation. Our data shows that CIAP-resistance was abolished by denaturation, and thus, CIAP-resistance depends on aggregated state of αsyn which shields αsyn's c-terminus from endogenous phosphatases. Resistance to dephosphorylation might account for PSER129 association with αsyn aggregates, and perhaps, similarly other αsyn PTMs. Several studies have implicated PSER129 as a mediator of αsyn aggregation (10, 13), but our results make it plausible, perhaps even likely, that the observed PSER129 accumulation in the synucleinopathy brain is an epiphenomenon. Exogenous fibrils when injected do not become phosphorylated(23), therefore endogenous non aggregated αsyn is likely phosphorylated prior to misfolding

and preserved by the conformational shift. Whether PSER129 has pathogenic relevance, or not is an open question but PSER129 remains a specific and valuable marker for αsyn pathology, and enzymatic pretreatments (i.e., CIAP or protease) especially in animal models, will enhance that specificity.

Our previous work found widespread regionally specific endogenous-PSER129 in the mammalian brain (6). Here we extend that finding to explain several phenomena. First, PSER129 content fluctuated greatly between specimens, with some brain specimens (e.g., rodent and human) showing little or no endogenous-PSER129. In addition, we observed what we called an “all-or-none” effect, where endogenous-PSER129 abundance was proportional across the entire neuroaxis for any given rodent brain. Here we demonstrate that the “all-or-none” effect is due to differences in the rapidity and completeness of PFA fixation, and not because of a global biological process driving endogenous-PSER129 in the brain. However, we did see evidence in well preserved brains that PSER129 acts as a proxy for neuronal activity, for example individual olfactory bulb glomeruli show varying PSER129 intensity (Fig. 1A,2B), consistent with odorant activation around the time of perfusion(24, 25). Second, our results clarify why there is a lack of endogenous-PSER129 observed in the human brain(6). Immersion fixation does not preserve endogenous-PSER129 due to limited rate of formalin diffusion, and therefore, there is a low probability of detecting endogenous PSER129 in human post-mortem brain even when PMIs are short and tissue volumes are small (6). Third, rapid dephosphorylation of PSER129 occurs in tissue lysates(2), but our findings show that PSER129 is also rapidly dephosphorylated intracellularly following death. Therefore, it is likely that a post-mortem artifact has led to the conclusion that PSER129 is specific for αsyn pathology. Fourth, in several mammalian cell types in the brain (e.g., mitral cells) we find endogenous-PSER129 to be abundant, and in OB-PFF mice, capable of obscuring aggregated-PSER129 detection (Fig. 3). Our results demonstrate the distinction between endogenous non-aggregated and aggregated-PSER129 is critical in these models.

Several practical applications result from these studies. First, rapid (<5 min) complete perfusion fixation was a critical parameter for preserving endogenous-

PSER129 similar to what has been observed with other phosphoepitopes(17). Therefore, studies looking at endogenous PSER129 should ensure proper fixation, and remove animals where perfusion failed or immersion fixation was used, should be eliminated from analysis. Although not tested here, timely flash freezing, or lysis in phosphatase inhibitor buffer also can preserve endogenous-PSER129(5, 16). To detect aggregated-PSER129 perfusion was less critical, and delayed fixation may be preferred in some instances because it removes potentially unwanted endogenous PSER129 signal. Second, to differentiate endogenous- vs. aggregated-PSER129 in pre-clinical animal models, CIAP pretreatment may be useful. Protease pretreatment (e.g., PK, Trypsin, GluC) could also be used (Figure S1), but those treatments are destructive (in particular PK) and can impede downstream assays (e.g., peptide identification by mass spectrometry). For this reason, CIAP pretreatment might be a particularly valuable approach to increase specificity for aggregated-PSER129 in multiple assay platforms. Endogenous-PSER129 is CIAP sensitive, and aggregated-PSER129 is enzyme insensitive, this simple observation might help differentiate the two pools in future studies. As we found previously(6), dilution of EP1536Y is critical for both IHC and western blot to avoid non-specific binding. Dilutions below 1:10,000 for extended incubation periods (e.g., overnight) are dominated by interfering non-specific signal (i.e., observed in αsyn knockouts)

These studies have several limitations. First, we cannot conclude a precise mechanism for the observed loss of PSER129 epitope, although post-mortem enzymatic dephosphorylation or proteolysis likely account for our observations. Because we did not observe a reduction in total αsyn with postmortem interval (Fig. 1) endogenous phosphatases are likely responsible, but limited C-terminal truncation or ancillary PTMs near the PSER129 epitope is also possible(16). Interestingly, post-mortem PSER129-loss was cell compartment specific, with nuclear endogenous-PSER129 being least sensitive to postmortem interval (Fig. 1) and corresponding with detection of high molecular weight endogenous-PSER129 (Fig. 1). Although specificity of these high molecular weight PSER129 species remain unclear(16), here we found they were sensitive to CIAP treatment (Fig. 4) and corresponded to high molecular weight αsyn, and therefore may represent high molecular weight nuclear endogenous-

PSER129. It is also important to note for protein extraction from fixed tissues, like done here, total protein monodispersion cannot be assumed(26). We previously observed that nuclear endogenous-PSER129 was partially protease resistant (6). This suggests nuclear PSER129 is folded, oligomerized, or interacting with yet unknown cellular components (i.e., proteins, nucleic acids, lipids). Of note, nuclear PSER129 accumulates in transgenic mice (27, 28), interestingly are seen prior to widespread aggregation(29), and therefore this modification might have particular significance for the nucleus, or cytosolic-nuclear translocation(30) in the early pathogenic process(31, 32). That said, cytosolic/perinuclear aggregated-PSER129 is the prominent presentation of pathology in PD brain, nuclear alpha-synuclein accumulation is controversial(33), and cytosolic aggregation inhibits PSER129 mediated translocation to the nucleus.(33)

In summary, aggregated-PSER129 resists dephosphorylation which may account for apparent enrichment in pathological aggregates. Endogenous non aggregated-PSER129 can be rapidly dephosphorylated and differentiated from aggregated-PSER129 by pretreatment of specimens with CIAP. Critical parameters to measure endogenous non aggregated-PSER129 include 1) tissue preparation 2) primary antibody dilution and 3) detection system sensitivity. Endogenous non aggregated-PSER129 may have some significance particularly in the nucleus of neurons. This work helps define and differentiate two distinct PSER129 populations in the brain. Furthermore, our results have important implications for the role of PSER129 in pathogenesis.

Materials and Methods

Tissue specimens

C57BL/6J male and female mice (n=24) 4-8 months of age and 4–6-month-old male homozygous B6;C3-Tg(Prnp-SNCA*A53T)83Vle/J (M83) mice (n=2) were used. All animal procedures were reviewed and approved by the Rush University Medical Center institutional animal care and use committee. Human brain tissues were acquired through the Rush Movement Disorders brain bank and 40-micron floating sections prepared as previously described(34).

PFF injections

Wild-type B6 mice (n=3) were stereotactically injected with 5 micrograms of human αsyn preformed fibrils (PFFs) into the granular layer of the olfactory bulb (coordinates: coordinates: AP, +5.4 mm; ML, +/− 0.75 mm; DV, −1 mm relative to bregma and dural surface) or PBS and euthanized two months following injection as previously described(20, 22). All fibril preparations had been prepared, sonicated, aliquoted, frozen and then stored at –80°C. Prior to injection, aliquots were thawed at 37°C for 3 mins, briefly sonicated, then injected into the OB(35).

Tissue preparation and Perfusion

Animal tissues were collected by either anesthetizing with ketamine/xylazine (100 mg Ketamine/ kg and 10 mg xylazine / kg), or euthanizing via C02, and then transcrardially perfusing with PBS until the perfusate exiting a small incision in the right atrium was clear. All animals were perfusion fixed, but perfusion fixation was delayed for some animals, by first clearing blood with PBS and then waiting 30-min (n=4) or 1-hr (n=4) prior to perfusion with 4% PFA. Rapidly perfused mice (n=2, “optimal”) were quickly flushed with ice-cold PBS (<20s) and then immediately perfused with ice cold 4% PFA. All mice in PFF studies were perfusion fixed by standard methods(36). Whole brain specimens were removed and post-fixed in 4% PFA at 4°C overnight. M83 mouse brains were immersion fixed for 3-days at 4°C. Brains were then equilibrated in 15% and then 30% sucrose solutions. Brain specimens were then frozen and sectioned to 40-micron thickness on a freezing stage microtome. Sections were stored in cryoprotectant solution (30% sucrose, 30% ethylene glycol in PBS) at -20°C.

Calf Intestine Alkaline Phosphatase (CIAP) treatment

Tissue sections matched for level from each animal were washed three times in dilution media (DM, 50mM Tris-HCl pH 7.2, 150 mM NaCl, 0.05% Triton-X100) and then incubated with 1% Triton X-100 in DM for 10 minutes. Tissues were then incubated with CIAP for 1 hour at 37°C using CIAP buffer (100 mM NaCl, 10 mM MgCl2, and 50 mM Tris-HCl at pH 7.9) containing 600 units of the CIAP enzyme (Promega). Tissues were then washed in DM and heat-induced antigen retrieval (HIAR) was performed by using

sodium citrate buffer (10 mM sodium citrate, 0.05% Tween 20, and pH 6.0) at 95°C for 20 minutes, and then tissues were then cooled to room temperature.

Immunohistochemistry

Free-floating mouse brain sections were rinsed in dilution media (DM, 50mM Tris-HCl pH 7.4, 150mM NaCl, 0.5% Triton-X100) and incubated in peroxidase quenching solution (0.3% hydrogen peroxide, 0.1% sodium azide) containing blocking buffer (3% goat serum, 2% BSA, 0.4% Triton X-100 in DM) for 1 hour at room temperature. Sections were washed in DM and incubated with PSER129 antibody (Abcam, “EP1536Y”, 1:50,000 diluted in blocking buffer) overnight. The next day, tissues were washed and incubated with biotinylated anti-rabbit antibody (Vector Laboratories, dil. 1:200 in blocking buffer) for 1 hour at room temperature, followed by rinsing in DM. The sections were then incubated with prepared elite avidin-biotin complex (ABC) reagent (Vector Laboratories) for 75 min at room temperature. For tyramide signal amplification (TSA) sections were washed in DM and borate buffer (0.05M Sodium Borate, pH 8.5). Samples were then incubated with TSA reaction buffer (1 µg / mL biotinyl tyramide, 0.003% hydrogen peroxide in borate buffer) for 30 minutes and at room temperature. Following the TSA reaction, samples were rinsed in DM and heated to 95°C in citrate buffer for 20 minutes, cooled, and incubated with ABC reagent for 75 minutes at room temperature. Some samples were stained without TSA. Tissues were developed using a standard nickel-enhanced 3,3'-diaminobenzidine (DAB)-imidazole protocol and rinsed with sodium acetate buffer (0.2 M Imidazole, 1.0 M sodium acetate buffer, pH 7.2) and PBS before mounting on glass slides. Sections were counterstained with methyl green, dehydrated, cleaned with xylenes, and cover-slipped with cytosol 60 (Fisher Scientific).

Protein extraction

Proteins were extracted from free floating PFA fixed tissues sections as previously described (6, 34). Briefly, sections were rinsed in DM several times, collected into a 1.5mL Eppendorf tube, and then heated to 98°C in reversal buffer (0.5M Tris-HCl pH 8.0, 5% SDS, 150mM NaCl, 2mM EDTA) for 30 min. Samples were vigorously vortexed and heated for an additional 15 min. After cooling to room temperature

samples were centrifuged at 22,000 x g for 20 min at room temperature. The supernatant was carefully collected, and BCA assay performed on 0.5µl of extract to determine protein concentration.

Western blotting

15-20 µg of protein were separated using 4-13% Bis-tris gels, blotted onto methanol-activated polyvinylidene difluoride (PVDF) membrane, post-fixed with 4% PFA for 30 min, and then allowed to dry completely. Blots were then reactivated in methanol and stained for total protein (Licor). For CIAP treatment, blots were blocked in 2% (w/v) polyvinylpyrrolidone (PVP) for 1h, and then incubated with CIAP as described above. Blots were then rinsed with TBST (20 mM Tris-HCl pH 7.6, 150 mM NaCl, 0.1% Tween-20) and placed in blocking buffer (TBST and 5% BSA or 5% dry milk) for 1 h at room temperature. Blots were incubated overnight with PSER129 diluted 1:50,000 or SYN1 diluted 1:2000 in blocking buffer. Blots were then washed and incubated with anti-rabbit HRP conjugate (dil. 1:20,000, Invitrogen), anti-mouse HRP conjugate (dil. 1:6,000, Cell signaling), or anti-mouse IRDye 680RD (dil. 1:20,000 Li-Cor) diluted in blocking buffer for 1 h. Membranes were washed again in TBST and imaged using enhanced chemiluminescence (ECL) substrates (Bio-Rad, product # 170-5060 or ThermoFisher Scientific, product #38554) with a Chemidoc imager (Bio-Rad) or odyssey M imager for fluorescence (Li-Cor).

Microscopy and imaging

Prepared slides were imaged with Nikon A1 inverted microscope using a 10X, 20X or 63X objective. Whole section scans were acquired with either the Nikon A1 microscope with 10X objective, or the Odyssey-M whole slide imaging functionality. Whole section scans were imported into adobe photoshop for downsizing, cutting, auto-color balancing, and auto-brightness adjustments. Edited images were imported into adobe illustrator for arrangement and final presentation in figures.

Data analysis and figures

DAB-stained tissues were quantified using Nikon Elements software. Western blot quantification was performed using Emperia studio 3.0 (Li-Cor) and ImageJ.

Statistical analysis and graphing were performed using GraphPad Prism. To compare experimental groups, we used One-way ANOVA with Dunnet's or Tukey post-hoc tests. Pearson correlation was also performed.

Figure Legends

Figure 1. PSER129 detection requires rapid perfusion fixation. Mice were euthanized by CO2 inhalation, and blood cleared by transcadial perfusion with PBS. Following a delay of 30 or 60 min, mice were then perfused with 4% PFA. (A) PSER129 staining across the neuroaxis. (B) High magnification images of PSER129 staining in select brain regions. (C) Proteins extracted from sections across the neuroaxis were resolved by SDS-PAGE and blotted. Blots were probed for total protein (Revert protein stain, Licor), αsyn, and PSER129. Quantification of total αsyn (C), total PSER129 (D), ratio of PSER129 to αsyn. All sections developed with nickel-DAB Chromogen (black/purple) and counterstained with methylgreen. OB = olfactory bulb, AMYG = amygdala, Nac = nucleus accumbens, HIP = Hippocampus, GP = Globus pallidus, HYPO = hypothalamus, SNPr = substantia nigra pars compacta, MCL = mitral cell layer, GCL = granular cell layer, EC = entorhinal cortex. n=2-4. ***ANOVA, Dunnett's post-hoc test. p>0.01. Scale bar = 25µm.

Figure 2. Anesthetics did not influence PSER129 abundance in the brain. n=4-5. Mice were euthanized by CO2 inhalation, and then rapidly fixed by transcadial perfusion with PBS followed by 4% PFA. Ten minutes prior to euthanasia, some animals were exposed to xylazine (XYL, 10mg/kg) or ketamine (KET, 100mg/kg). Brain sections across the neuroaxis were stained for PSER129. (A) PSER129 staining in OB sections. (B) Proteins extracted from sections across neuroaxis were resolved by SDS-PAGE and blotted. Blots were probed for total protein (B, top panel), αsyn, and PSER129. Quantification of total αsyn (C), total PSER129 (D), ratio of PSER129 to αsyn (E), and (F) correlation between αsyn and PSER129 content. No significant differences were found between experimental groups (One-way ANOVA, Tukey's post-hoc). Total asyn did not correlate with total PSER129 (Pearson Correlation, $R^2 = 0.01045$). All sections developed with nickel-DAB Chromogen (black/purple) and counterstained with methylgreen. n=4-5.

Figure 3. Aggregated-PSER129 is phosphatase resistant. Mice were bilaterally injected with either PBS or PFFs into the OB GCL. Two months following injection, animals were euthanized with a mixture of ketamine/xylazine followed by transcardial perfusion fixation. Brain sections across the neuroaxis were stained for PSER129 with and without CIAP pretreatment. (A) Whole section images of PSER129 stained brain images across the neuroaxis, with (+CIAP) or without CIAP (-CIAP) pretreatment. (B) Low and (C) high magnification images of select brain regions. OB = olfactory bulb, AMYG = amygdala, Nac = nucleus accumbens, HIP = Hippocampus, GP = Globus pallidus, HYPO = hypothalamus, SNPr = substantia nigra pars compacta, MCL = mitral cell layer, GCL = granular cell layer, EC = entorhinal cortex. All sections developed with nickel-DAB Chromogen (black/purple) and counterstained with methylgreen. n=3.

Figure 4. Human brain αsyn pathology is phosphatase resistant. (A) Whole section images of transverse midbrain sections from (A) PD and (B) MSA cases stained for PSER129 with (+CIAP) or without (-CIAP) CIAP pretreatment. High magnification images of substantia nigra of (C) PD and (D) MSA. (E) Quantification of staining in PD and MSA brain with or without CIAP. (F) Proteins extracted tissues that have or did not have αsyn aggregates. Proteins were separated by SDS-PAGE and blotted onto PVDF membranes which were incubated with and without CIAP. Blots were probed for both PSER129 and αsyn. All sections developed with nickel-DAB Chromogen (black/purple) and counterstained with methylgreen n=2-3

References

1. Koga S, Sekiya H, Kondru N, Ross OA, & Dickson DW (2021) Neuropathology and molecular diagnosis of Synucleinopathies. *Molecular Neurodegeneration* 16(1):83.
2. Fujiwara H*, et al.* (2002) alpha-Synuclein is phosphorylated in synucleinopathy lesions. *Nat Cell Biol* 4(2):160-164.
3. Manzanza NO, Sedlackova L, & Kalaria RN (2021) Alpha-Synuclein Post-translational Modifications: Implications for Pathogenesis of Lewy Body Disorders. *Front Aging Neurosci* 13:690293.
4. Mahul-Mellier AL*, et al.* (2020) The process of Lewy body formation, rather than simply alpha-synuclein fibrillization, is one of the major drivers of neurodegeneration. *Proc Natl Acad Sci U S A* 117(9):4971-4982.
5. Ramalingam N*, et al.* (2023) Dynamic physiological α-synuclein S129 phosphorylation is driven by neuronal activity. *npj Parkinson's Disease* 9(1):4.
6. Killinger BA*, et al.* (2023) Distribution of phosphorylated alpha-synuclein in non-diseased brain implicates olfactory bulb mitral cells in synucleinopathy pathogenesis. *npj Parkinson's Disease* 9(1):43.
7. Parra-Rivas LA*, et al.* (2022) Serine-129 phosphorylation of α-synuclein is a trigger for physiologic protein-protein interactions and synaptic function. *bioRxiv*:2022.2012.2022.521485.
8. Machiya Y*, et al.* (2010) Phosphorylated alpha-synuclein at Ser-129 is targeted to the proteasome pathway in a ubiquitin-independent manner. *J Biol Chem* 285(52):40732-40744.
9. Chau KY, Ching HL, Schapira AH, & Cooper JM (2009) Relationship between alpha synuclein phosphorylation, proteasomal inhibition and cell death: relevance to Parkinson's disease pathogenesis. *Journal of neurochemistry* 110(3):1005-1013.
10. Ghanem SS*, et al.* (2022) alpha-Synuclein phosphorylation at serine 129 occurs after initial protein deposition and inhibits seeded fibril formation and toxicity. *Proc Natl Acad Sci U S A* 119(15):e2109617119.
11. McFarland NR*, et al.* (2009) Alpha-synuclein S129 phosphorylation mutants do not alter nigrostriatal toxicity in a rat model of Parkinson disease. *Journal of neuropathology and experimental neurology* 68(5):515-524.
12. Azeredo da Silveira S*, et al.* (2009) Phosphorylation does not prompt, nor prevent, the formation of alpha-synuclein toxic species in a rat model of Parkinson's disease. *Hum Mol Genet* 18(5):872-887.
13. Karampetsou M*, et al.* (2017) Phosphorylated exogenous alpha-synuclein fibrils exacerbate pathology and induce neuronal dysfunction in mice. *Sci Rep* 7(1):16533.
14. Delic V*, et al.* (2018) Sensitivity and specificity of phospho-Ser129 alpha-synuclein monoclonal antibodies. *J Comp Neurol* 526(12):1978-1990.
15. Killinger BA*, et al.* (2023) Distribution of phosphorylated alpha-synuclein in non-diseased brain implicates olfactory bulb mitral cells in synucleinopathy pathogenesis. *NPJ Parkinsons Dis* 9(1):43.
16. Lashuel HA*, et al.* (2022) Revisiting the specificity and ability of phospho-S129 antibodies to capture alpha-synuclein biochemical and pathological diversity. *NPJ Parkinsons Dis* 8(1):136.
17. Wang Y*, et al.* (2015) Rapid alteration of protein phosphorylation during postmortem: implication in the study of protein phosphorylation. *Scientific Reports* 5(1):15709.
18. Mittal S*, et al.* (2017) beta2-Adrenoreceptor is a regulator of the alpha-synuclein gene driving risk of Parkinson's disease. *Science* 357(6354):891-898.
19. Cichon J*, et al.* (2023) Ketamine triggers a switch in excitatory neuronal activity across neocortex. *Nat Neurosci* 26(1):39-52.

20. Rey NL, *et al.* (2016) Widespread transneuronal propagation of alpha-synucleinopathy triggered in olfactory bulb mimics prodromal Parkinson's disease. *J Exp Med* 213(9):1759-1778.
21. Rey NL, Petit GH, Bousset L, Melki R, & Brundin P (2013) Transfer of human alpha-synuclein from the olfactory bulb to interconnected brain regions in mice. *Acta Neuropathol* 126(4):555-573.
22. Walton S, *et al.* (2023) Neither alpha-synuclein-preformed fibrils derived from patients with GBA1 mutations nor the host murine genotype significantly influence seeding efficacy in the mouse olfactory bulb. *bioRxiv*:2023.2008.2024.554646.
23. Courte J, *et al.* (2020) The expression level of alpha-synuclein in different neuronal populations is the primary determinant of its prion-like seeding. *Sci Rep* 10(1):4895.
24. Berkowicz DA, Trombley PQ, & Shepherd GM (1994) Evidence for glutamate as the olfactory receptor cell neurotransmitter. *J Neurophysiol* 71(6):2557-2561.
25. Wang IH, *et al.* (2022) Spatial transcriptomic reconstruction of the mouse olfactory glomerular map suggests principles of odor processing. *Nat Neurosci* 25(4):484-492.
26. Kawashima Y, Kodera Y, Singh A, Matsumoto M, & Matsumoto H (2014) Efficient extraction of proteins from formalin-fixed paraffin-embedded tissues requires higher concentration of tris(hydroxymethyl)aminomethane. *Clin Proteomics* 11(1):4.
27. Wakamatsu M, *et al.* (2007) Accumulation of phosphorylated alpha-synuclein in dopaminergic neurons of transgenic mice that express human alpha-synuclein. *J Neurosci Res* 85(8):1819-1825.
28. Schell H, Hasegawa T, Neumann M, & Kahle PJ (2009) Nuclear and neuritic distribution of serine-129 phosphorylated alpha-synuclein in transgenic mice. *Neuroscience* 160(4):796-804.
29. Bencsik A, Muselli L, Leboidre M, Lakhdar L, & Baron T (2014) Early and Persistent Expression of Phosphorylated α-Synuclein in the Enteric Nervous System of A53T Mutant Human α-Synuclein Transgenic Mice. *Journal of Neuropathology & Experimental Neurology* 73(12):1144-1151.
30. Pinho R, *et al.* (2019) Nuclear localization and phosphorylation modulate pathological effects of alpha-synuclein. *Hum Mol Genet* 28(1):31-50.
31. Kontopoulos E, Parvin JD, & Feany MB (2006) Alpha-synuclein acts in the nucleus to inhibit histone acetylation and promote neurotoxicity. *Hum Mol Genet* 15(20):3012-3023.
32. Schaser AJ, *et al.* (2019) Alpha-synuclein is a DNA binding protein that modulates DNA repair with implications for Lewy body disorders. *Sci Rep* 9(1):10919.
33. Koss DJ, *et al.* (2022) Nuclear alpha-synuclein is present in the human brain and is modified in dementia with Lewy bodies. *Acta Neuropathol Commun* 10(1):98.
34. Killinger BA, *et al.* (2022) In situ proximity labeling identifies Lewy pathology molecular interactions in the human brain. *Proc Natl Acad Sci U S A* 119(5).
35. Rey NL, *et al.* (2019) alpha-Synuclein conformational strains spread, seed and target neuronal cells differentially after injection into the olfactory bulb. *Acta Neuropathol Commun* 7(1):221.
36. Walton S, *et al.* (2023) Neither alpha-synuclein-preformed fibrils derived from patients with GBA1 mutations nor the host murine genotype significantly influence seeding efficacy in the mouse olfactory bulb. *bioRxiv*.

Figure 1

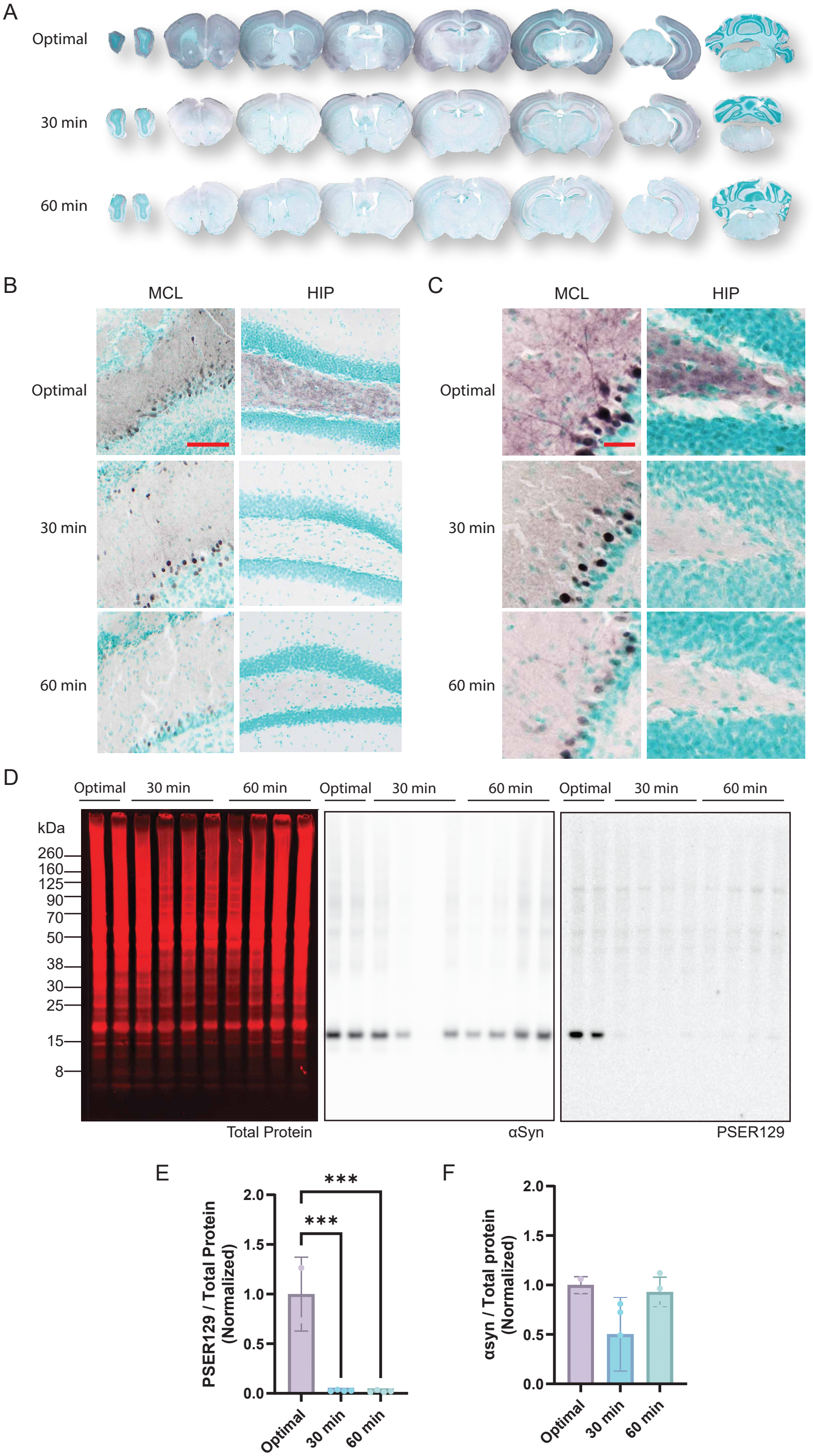
A
Optimal
30 min
60 min
B
MCL
HIP
Optimal
30 min
60 min
C
MCL
HIP
Optimal
30 min
60 min
D
Optimal
30 min
60 min
Optimal
30 min
60 min
Optimal
30 min
60 min
kDa
260
160
125
90
70
50
38
30
25
15
8
Total Protein
αSyn
PSER129
E
PSER129 / Total Protein (Normalized)
2.0
1.5
1.0
0.5
0.0
***
***
Optimal
30 min
60 min
F
αsyn / Total protein (Normalized)
2.0
1.5
1.0
0.5
0.0
Optimal
30 min
60 min

Figure 2

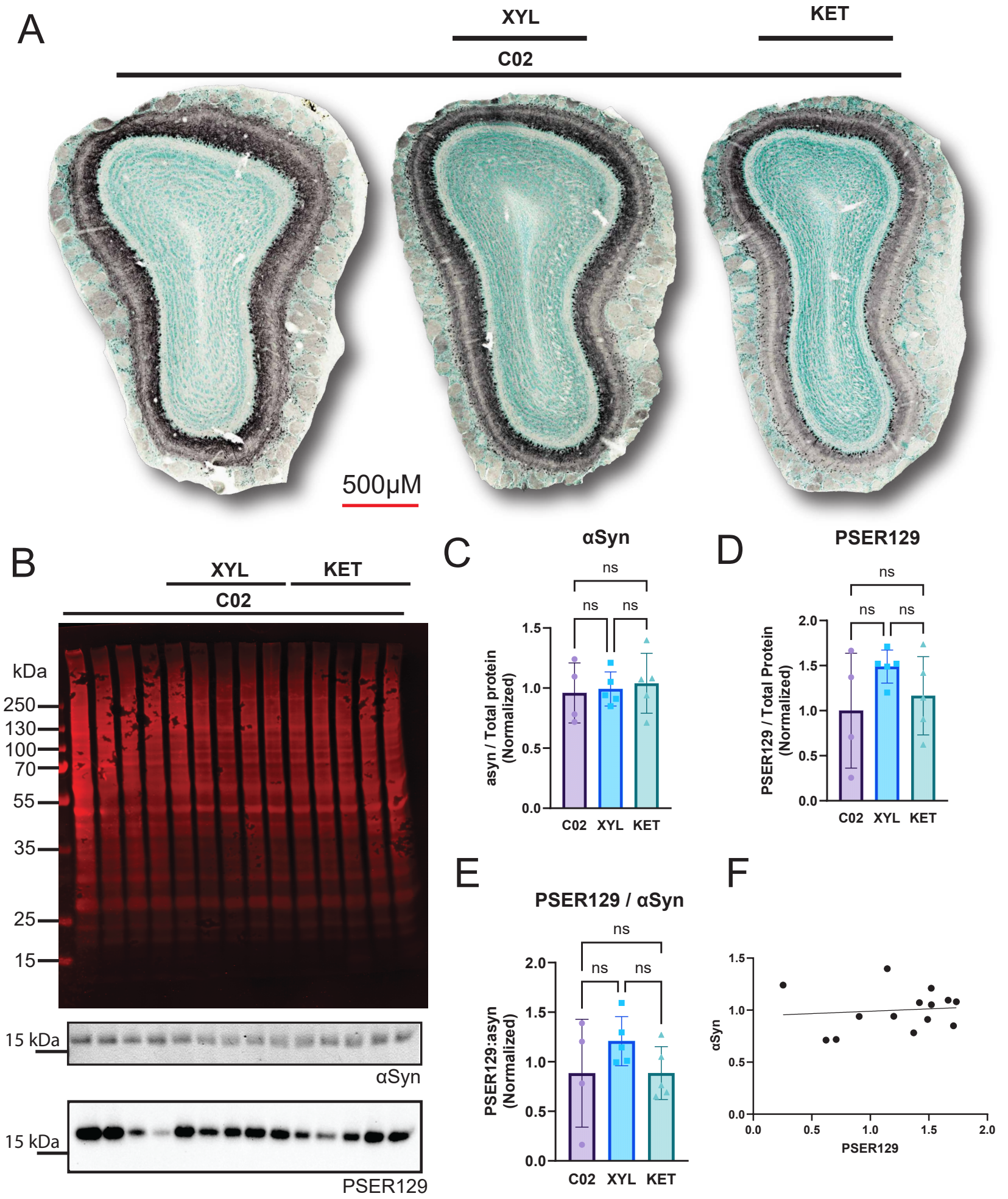
A
XYL
KET
C02
500µM
B
XYL
KET
C02
kDa
250
130
100
70
55
35
25
15
15 kDa
αSyn
15 kDa
PSER129
C
αSyn
ns
ns
ns
asyn / Total protein (Normalized)
1.5
1.0
0.5
0.0
C02
XYL
KET
D
PSER129
ns
ns
ns
PSER129 / Total Protein (Normalized)
2.0
1.5
1.0
0.5
0.0
C02
XYL
KET
E
PSER129 / αSyn
ns
ns
ns
PSER129:asyn (Normalized)
2.0
1.5
1.0
0.5
0.0
C02
XYL
KET
F
αSyn
1.5
1.0
0.5
0.0
0.0
0.5
1.0
1.5
2.0
PSER129

Figure 3

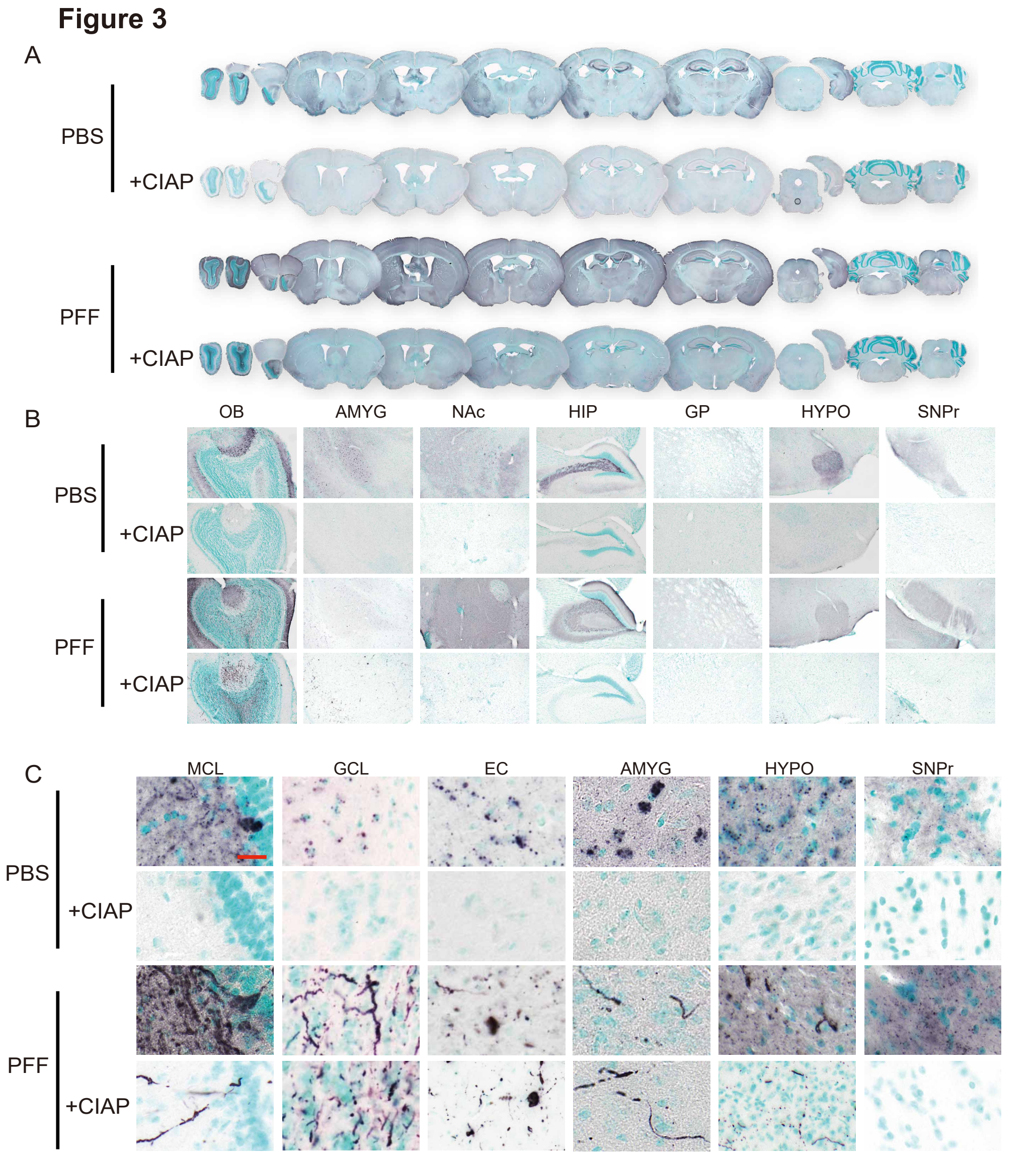
A
PBS
+CIAP
PFF
+CIAP
B
OB
AMYG
NAc
HIP
GP
HYPO
SNPr
PBS
+CIAP
PFF
+CIAP
C
MCL
GCL
EC
AMYG
HYPO
SNPr
PBS
+CIAP
PFF
+CIAP

Figure 4

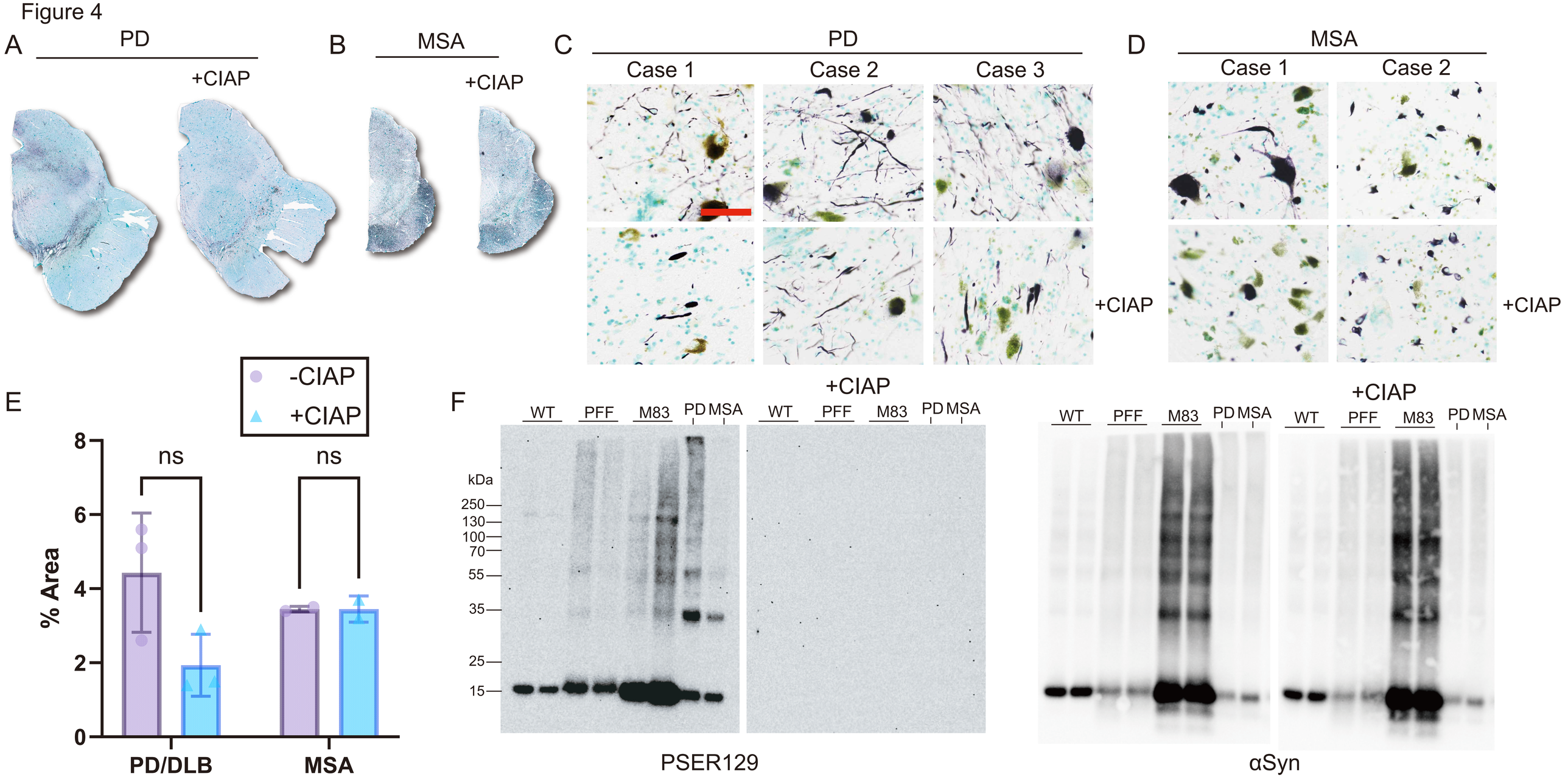
A
PD
+CIAP
B
MSA
+CIAP
C
PD
Case 1
Case 2
Case 3
+CIAP
D
MSA
Case 1
Case 2
+CIAP
E
-CIAP
+CIAP
ns
ns
% Area
0
2
4
6
8
PD/DLB
MSA
F
+CIAP
WT
PFF
M83
PD
MSA
kDa
250
130
100
70
55
35
25
15
PSER129
αSyn

A

Control
CIAP
GluC
Trypsin
Box 1
Box 2

B

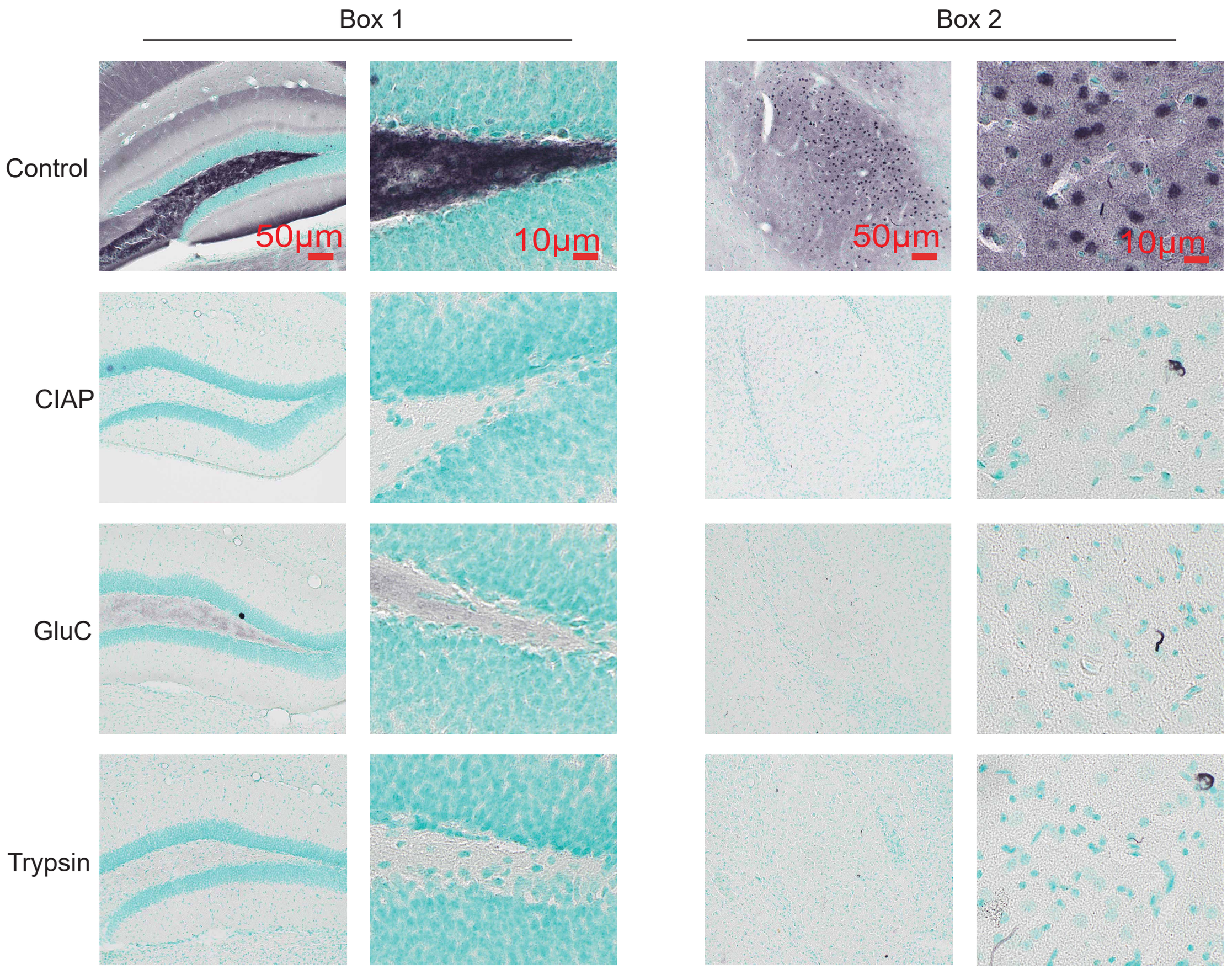
Box 1
Box 2
Control
CIAP
GluC
Trypsin
50μm
10μm
50μm
10μm

A

Control
CIAP + HIAR
CIAP + 0.3% SDS HIAR
CIAP + PK
Box 1
Box 2

B

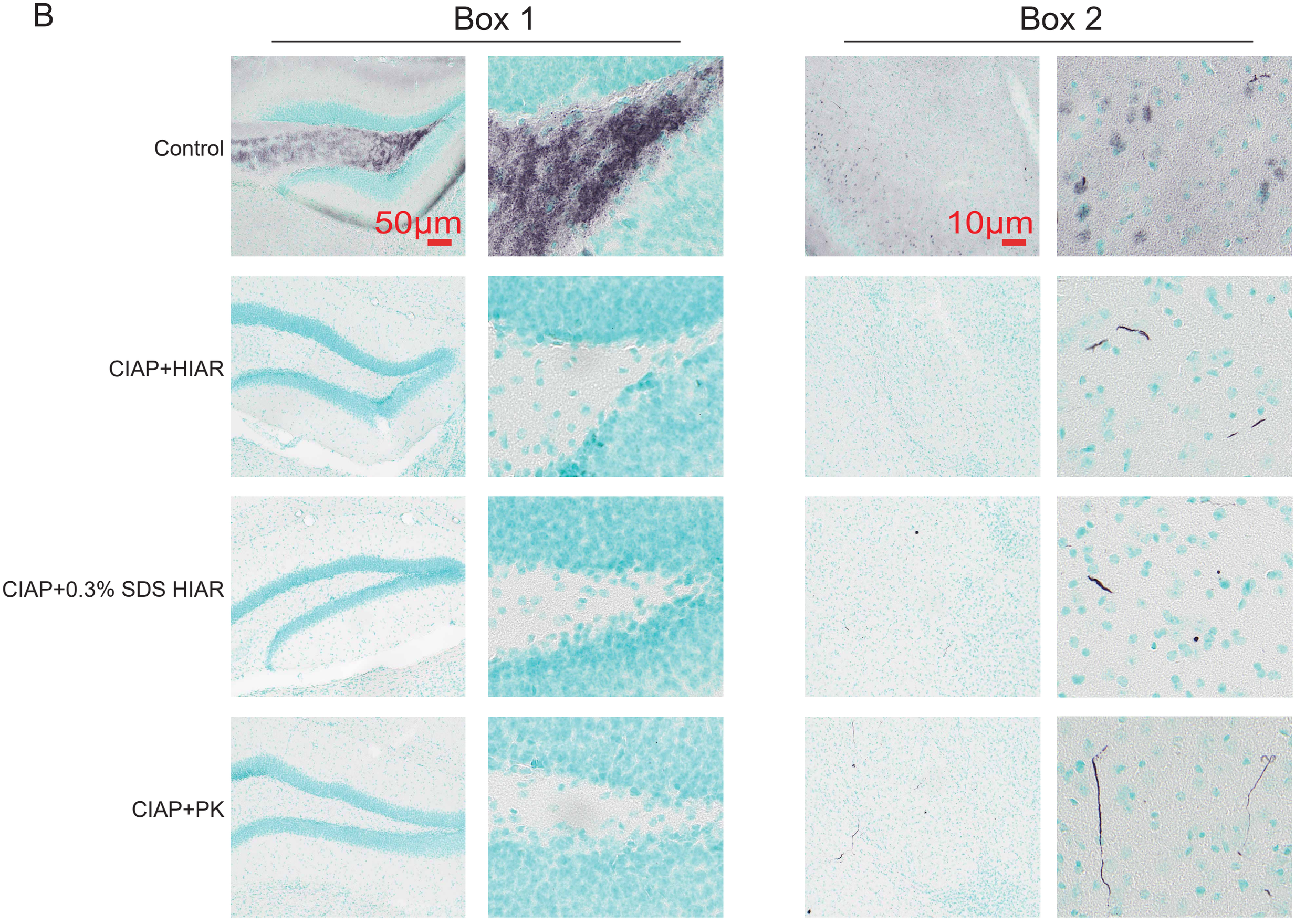
Box 1
Box 2
Control
CIAP+HIAR
CIAP+0.3% SDS HIAR
CIAP+PK
50μm
10μm